The EMBO Journal vol.9 no.10 pp.3067-3075, 1990

Ordered arrays of the photosystem I reaction centre after reconstitution: projections and surface reliefs of the complex at 2 nm resolution

Robert C.Ford[2], Andreas Hefti[1] and Andreas Engel[1]

Department of Biophysical Chemistry, Biocentre, University of Basel, CH-4056 Basel, Switzerland, and [1]M.E.Müller-Institute for High-Resolution Electron Microscopy at the Biocentre, University of Basel, CH-4056 Basel, Switzerland

[2]Present address: Department of Biochemistry and Applied Molecular Biology, UMIST, Manchester M60 1QD, UK

Communicated by J.Engel

We present an electron microscopical analysis of the photosystem I reaction centre, the membrane complex involved in the second light-driven step of photosynthetic electron transfer in plants and cyanobacteria. To this end, ordered two-dimensional arrays were reconstituted from detergent solubilized photosystem I reaction centres and phospholipids, and studied by electron microscopy and digital image processing. Small (P1) and large (P3) hexagonal lattices obtained with reaction centres of the thermophilic cyanobacterium *Phormidium laminosum* had unit cell sizes of a = b = 8.8 nm and 15.8 nm, respectively. Reaction centres of a second thermophilic strain, *Synechococcus* sp. OD24, gave square lattices (a = b = 14.5 nm; $P2_1$). Irrespective of the packing arrangement, projections of negatively stained photosystem I complexes showed elongated asymmetric shapes with a large domain at one end which was tilted with respect to a small domain forming the tip of the other end. Such features were also found in averaged projections of solubilized reaction centre trimers. Surface reliefs reconstructed from freeze-dried metal-shadowed $P2_1$ lattices revealed that reaction centres had a ridge of 2.5 nm height projecting from one side of the membrane while their other side was rather flat and exhibited a shallow, central indentation.

Key words: crystalline lipid-protein membranes/membrane protein/*Phormidium laminosum*/reaction centre/photosynthesis/photosystem/*Synechococcus* sp.

Introduction

The reaction centre of photosystem I is a membrane-bound protein complex which uses light energy to reduce ferredoxin and to oxidize plastocyanin in the photosynthetic electron transfer chain which is found in plants and cyanobacteria. The reduced ferredoxin, in turn, reduces NADP which is then used in various metabolic processes including the incorporation of carbon dioxide. The reaction centre from thermophilic cyanobacteria has been purified, and the trimeric complex crystallizes readily in the presence of polyethylene glycol and magnesium ions (Ford *et al.*, 1987, 1988; Witt *et al.*, 1988). It consists of at least four subunits, two of which are polytopic membrane proteins of molecular weight 83 kd (Fish *et al.*, 1985; Cantrell and Bryant, 1987). The two smaller subunits of molecular weights 15 and 10 kd can be removed by denaturation, leaving a partially active reaction centre (Takahashi *et al.*, 1982; Ford, 1987). The reaction centre is unusual in that it binds a large number (60-70) of light-harvesting molecules [chlorophyll (chl) *a* and carotenoid] in addition to the electron transfer components P700, A0, A1 and iron-sulphur centres X, A and B (Bengis and Nelson, 1975; Rutherford and Heathcote, 1985). This intriguing piece of engineering appears to be carried out almost entirely by the two large (83 kd) subunits, with the 10 kd subunit probably binding the two final iron-sulphur centres A and B (Hoj *et al.*, 1987; Ford, 1987). Although it is only the trimeric complex which crystallizes, it has become clear that it is the monomeric form which exists in the native cyanobacterial membranes (Morschel and Schatz, 1987; Ford and Holzenburg, 1988). Thus, there seems to be no physiological significance for the trimerization of the reaction centre.

Here we present the reconstitution of solubilized reaction centre trimers in the presence of dimyristoyl phosphatidylcholine (DMPC) into regular arrays. We have been able to produce different crystallographic two-dimensional (2-D) packing arrangements of the reaction centres from *Phormidium laminosum* and *Synechococcus* sp. in which one, two and three reaction centres were present per unit cell. Concomitant with the structural analysis of negatively stained or freeze-dried metal-shadowed crystalline reaction centre arrays by electron microscopy, absorption spectra and enzymatic activities were measured. We observed a retention of the native absorption spectrum and biological activity. These crystalline membrane arrays represent the basis for further structural and functional studies.

Results

As documented in Figure 1, negatively stained solubilized trimeric photosystem I (PSI) reaction centre complexes exhibited a triangular shape with a characteristic handedness and a diameter of 19.7 ± 1.1 nm (see Ford and Holzenburg, 1988). These features emerged strongly in the averaged projection from 80 well preserved trimers exhibiting stain boundaries between the complexes (Figure 1, insert). It revealed an elongated reaction centre of 13.7 nm length and 7.8 nm width being composed of a large and a small domain. Both domains had a triangular shape and were separated by a distinct groove running at an angle of ~45° with respect to the long axis of the complex. The large domain appeared to be further subdivided into a larger and a smaller subunit, the small subunit forming one tip of the reaction centre. Averages from different data sets containing 40 particles each showed Fourier ring correlation coefficients above background (Saxton and Baumeister, 1982) up to a spatial frequency of $(2.8\ nm)^{-1}$. While the majority of well preserved trimers exhibited the same handedness (see Figure

1), some particles had no distinct internal fine structure. In an attempt to identify top and bottom views, particles with no internal fine structure were aligned on the basis of their border and averaged. Alternatively, particles with opposite handedness were searched for and aligned by using the mirror image of the average shown in Figure 1 as reference.

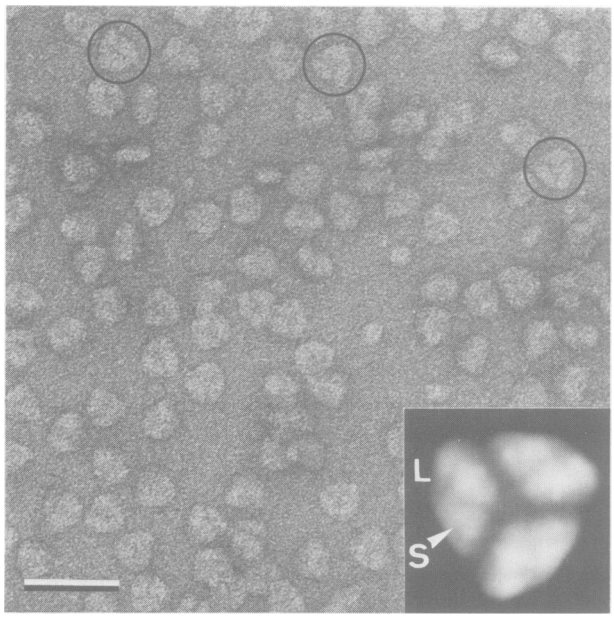

Fig. 1. Dodecyl maltoside-solubilized photosystem I reaction centres from *P.laminosum* can be separated into a monomeric and a trimeric fraction. Negatively stained reaction centre trimers displayed either a rectangular or a triangular shape with a distinct handedness as documented by well preserved units such as those marked with circles. After angular and translational alignment 80 such trimers were averaged and symmetrized to unveil the substructure of the reaction centre comprising a large (L) and a small (S) morphological subunit (insert). The scale bar represents 50 nm.

Both approaches failed to generate an averaged projection with reproducible features and opposite handedness. This may suggest that the trimers adsorbed preferentially in one orientation to the glow discharged grids, with their three-fold axis oriented perpendicularly to the carbon film, or that particles adsorbed in the other orientation provided insufficient contrast to be correctly aligned.

Dialysis of a mixture containing solubilized trimeric PSI reaction centre complexes and DMPC against various detergent-free buffers led to the formation of vesicles densely packed with particles. This was achieved with several commonly used detergents such as dodecyl maltoside, β-octylglucoside, octyl-polyoxyethylene and sodium deoxycholate (DOC). The size and shape of the particles indicated that once in the membrane the reaction centre was in its monomeric form, but there was no indication of crystallinity despite the dense packing. The dissociation of the trimeric complexes occurred upon reconstitution in all of the experiments that were performed under a variety of conditions.

With the detergent octyl-β-D-thioglucopyranoside (OBTG) however, ordered 2-D crystalline arrays were produced from PSI reaction centres and DMPC. With *P.laminosum* reaction centres, two types of hexagonal lattices assembled, depending on the $MgCl_2$ concentration. We adjusted the dialysis time to 60 h based on our experience from other reconstitution experiments. The temperature profile (see Materials and methods) was rather critical, as crystallinity was worse when the dialysis started directly at 37°C or when the temperature remained at 25°C during the entire experiment. At a concentration of 50 mM, the lattice vectors had a length of $a = b = 8.8 \pm 0.3$ nm (Figure 2), and formed an angle of $60.0 \pm 1.0°$. This hexagonal geometry was surprising, as the unit cell was just large enough to accommodate a single PSI reaction centre of the size determined from solubilized trimers shown in Figure 1. At $MgCl_2$ concentrations of 100−150 mM the small

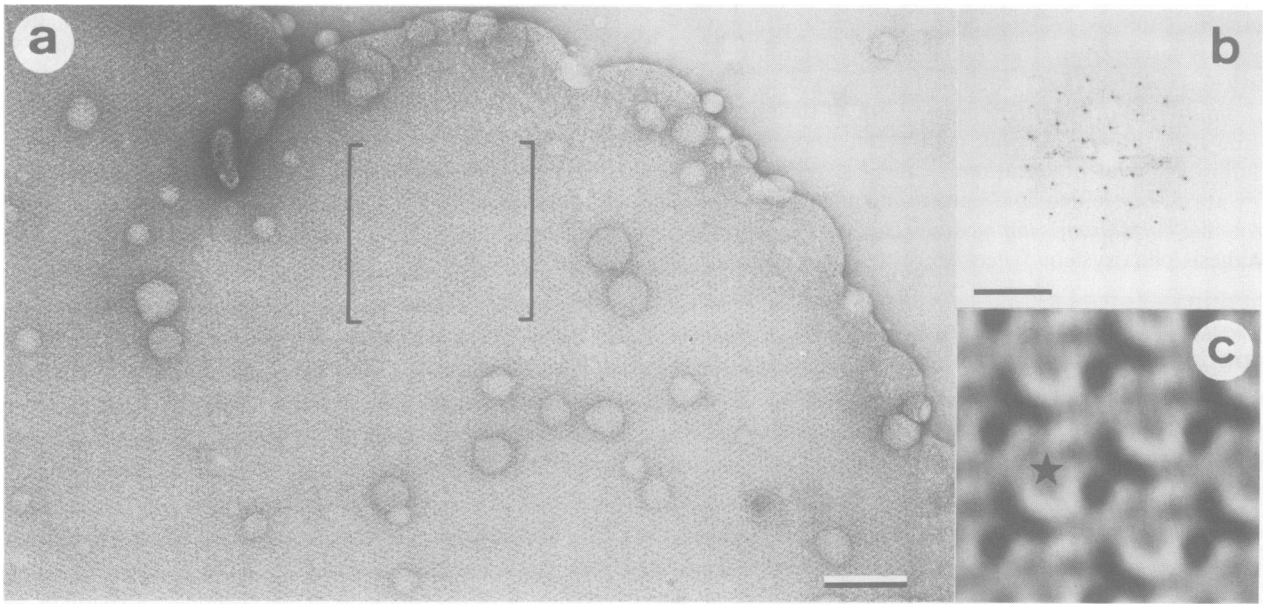

Fig. 2. Solubilized *P.laminosum* reaction centres were reconstituted into hexagonal 2-D arrays in the presence of lipids by dialysis of the detergent OBTG. At a $MgCl_2$ concentration of 50 mM, unit cells had a side length of 8.8 nm, providing just enough space for a single reaction centre (**a**). The hexagonal diffraction pattern from the area in brackets showed (3,1) order spots (**b**), indicating a resolution of $(2.1\ nm)^{-1}$. Unit cells (**c**) disclosed a rather round protein complex framed by deeply stained three-lobed pits, which had one prominent and two small protrusions bordering a shallow central indentation (*). The scale bars represent 100 nm in (a) and $(3\ nm)^{-1}$ in (b).

hexagonal lattice was still predominant, but patches of a larger hexagonal lattice were sometimes observed (Figure 3). The diffraction patterns as well as the averaged projections of small hexagonal lattices could vary distinctly from one lattice to another, but common features allowed averages to be separated into several classes which were observed for $MgCl_2$ concentrations of 50−150 mM. In all cases averaged projections showed an asymmetric unit cell morphology. The first class exhibited elongated complexes with a large and a small domain (Figure 3c) that correlated with the large and small domain of the reaction centre in the trimeric complex (Figure 1, insert). The second class disclosed strongly stained three-lobed pits separated by a structure consisting of three unequal protrusions embracing a shallow, slightly stained indentation (Figure 2c,*). In addition, further unit cell morphologies could be interpreted as multi-layered lattices which were stacked in identical angular orientation (data not shown). Diffraction patterns of these P1 lattices frequently showed (3,1) or (4,0) orders (Figures 2b and 3b) indicating a resolution of 2.1 nm and 1.9 nm, respectively, as confirmed by Fourier ring correlation functions calculated from the transforms of two independent correlation averages.

Above a $MgCl_2$ concentration of 200 mM, large hexagonal lattices were almost exclusively observed ($a = b = 15.8 \pm 0.6$ nm), exhibiting doughnut-shaped units with a diameter of 14.1 ± 0.7 nm and a distinct three-fold symmetry (r.m.s. deviation <6%) which appeared to consist of three reaction centre complexes (Figure 4a, upper part, Figure 4b). In contrast to the detergent solubilized triangular complexes (Figure 1, insert), the trimeric PSI doughnuts disclosed a hexagonal outline. This suggested a different association of the monomeric reaction centre with the exterior walls of the solubilized PSI trimer at the interior of the hexagonal doughnut. Nevertheless, the mass distribution of a single reaction centre had common features with that of the solubilized trimer, i.e. an elongated shape exhibiting a large and a small domain.

Frequently, such layers were stacked in identical angular orientation yielding Moiré patterns (Figure 4a, lower part) with a pronounced two-fold symmetry, as illustrated by the diffraction pattern (Figure 4c) as well as the averaged projection (Figure 4d). Prominent (4,1) diffraction orders indicated a resolution of 3.0 nm. Provided that the number of layers and their shift vectors with respect to one another are known, the single-layer motif can be extracted (Kühlbrandt, 1988). We examined this possibility under the assumption that the layers were stacked with a fixed displacement between adjacent layers (cf. Materials and methods) and found that between two and four layers could be superimposed with a shift approximately parallel to one lattice vector by half a unit cell. Theoretically, this should lead to the extinction of half of the diffraction spots for an even number of layers, a situation which was not observed in practice suggesting unequal staining of the different layers.

2-D lattices could readily be produced in membranes reconstituted from *Synechococcus* sp. reaction centres and DMPC in the presence of OBTG. Multi-layered square lattices exhibiting a lattice constant of 14.5 ± 0.8 nm formed with a buffer containing 50 mM $MgCl_2$, 20 mM HEPES, pH 7 (Figure 5a). These mosaic patches, although rather small, were sufficiently well ordered to yield diffraction spots to a resolution of 2.3 nm (Figure 5b). As documented by the unsymmetrized correlation average in Figure 5c, one unit cell housed two reaction centres that were related by a two-fold screw axis in the plane of the membrane, in accord with systematic attenuation of diffraction orders (h,0) for $h = 2n + 1$ (Figure 5b). It should be noted that a subtle but distinct difference in the average contrast of every other row in Figure 5a indicated different staining for top and

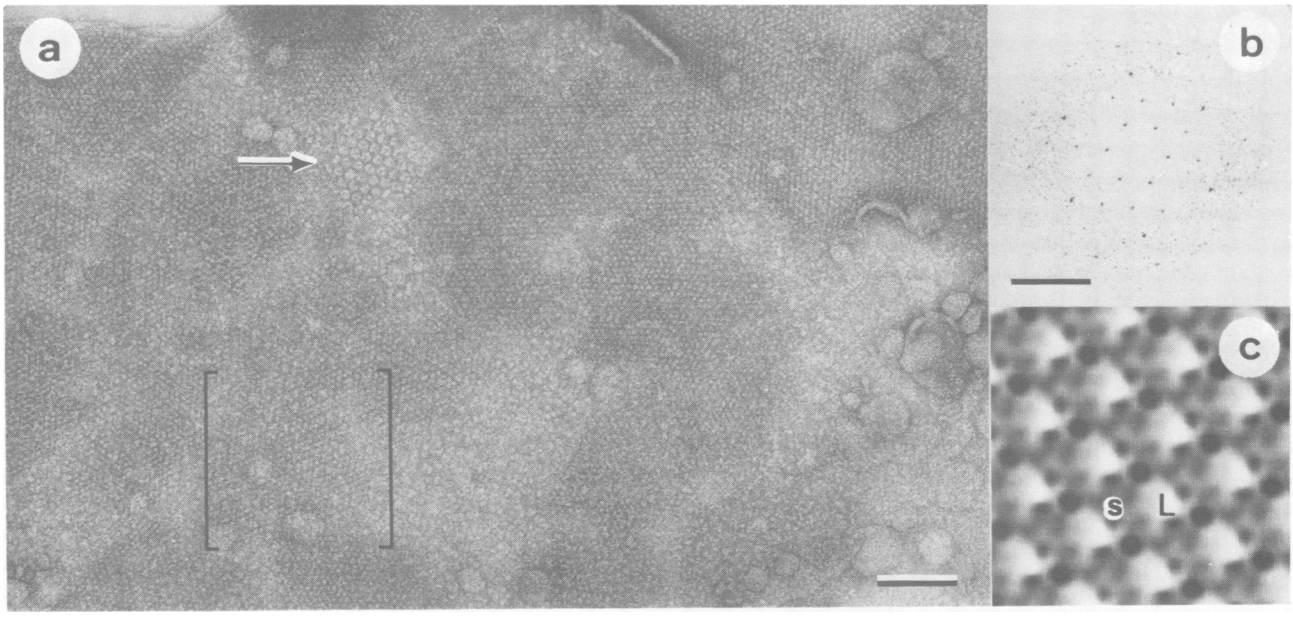

Fig. 3. At $MgCl_2$ concentrations of 100−150 mM, two *P.laminosum* reaction centre crystal forms co-existed, one exhibiting a lattice constant of 8.8 nm (brackets) and the other with unit cell dimensions $a = b = 15.8$ nm (arrow). Mosaic patches were connected by lipid bilayer areas which either contained less densely packed, disordered reaction centres or were protein-free. The hexagonal diffraction pattern from the area in brackets revealed (4,0) order spots (**b**), indicating a resolution of $(1.9\ nm)^{-1}$. The unit cell of the 8.8 nm lattice housed one elongated complex that had a large (L) and a small (S) domain (**c**). The scale bars represent 100 nm in (**a**) and $(3\ nm)^{-1}$ in (b).

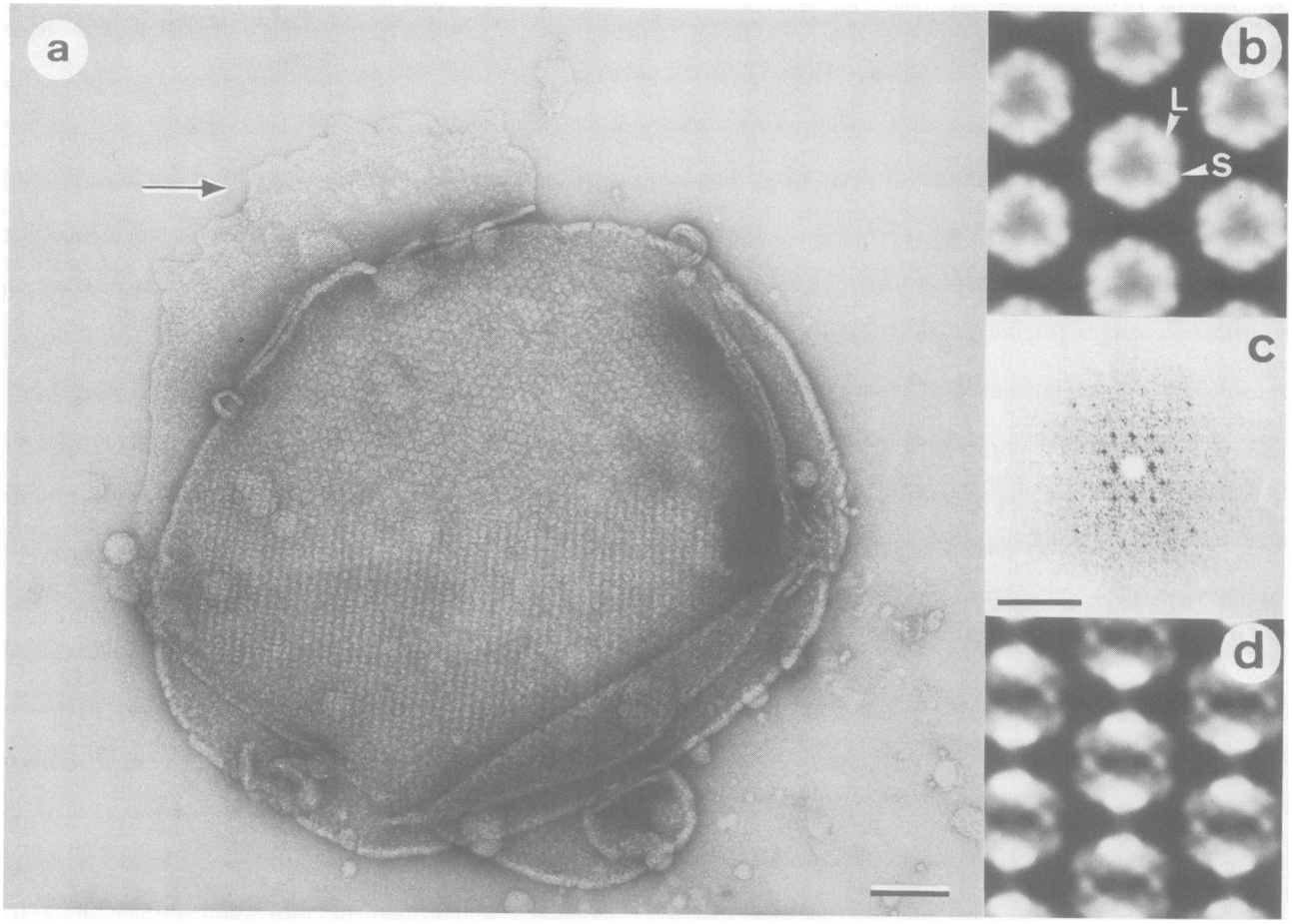

Fig. 4. Hexagonal lattices with unit cell dimensions a = b = 15.8 nm were assembled from *P.laminosum* reaction centres at $MgCl_2$ concentrations of 200–250 mM (**a**). Doughnut-shaped units (upper part) were discernible on single-layered lattices or when lattices were stacked in register, whereas vertical strings of morphological units were visible due to the superposition of lattices shifted with respect to each other by half a unit cell (lower part). Frequently, membranes that were much less densely packed with protein were associated with the vesicles (arrow). The doughnut-shaped units possessed a three-fold symmetry which has been enhanced in the average shown in (**b**) to disclose the reaction centre with its large (L) and small (S) morphological subunit. The diffraction pattern (**c**) as well as the correlation average (d) of the triple-layer lattice exhibited a two-fold symmetry. The scale bars represent 100 nm in (a) and $(3\ nm)^{-1}$ in (b).

bottom surfaces of the square lattice. This was also reflected by the weak (1,0) diffraction order in Figure 5b, as well as by the asymmetry of the contours displayed in Figure 7a documenting a minor deviation from $P2_1$ symmetry. *Synechococcus* sp. complexes showed a pronounced asymmetry similar to that of projections from *P.laminosum* reaction centres presented above.

In order to establish the topography of the reaction centre top and bottom surfaces, the $P2_111$ lattices assembled from *Synechococcus* sp. PSI complexes were freeze-dried and metal shadowed with tantalum–tungsten (Figure 6a). Thus prepared lattices showed a regular surface modulation due to a single prominent elevation per unit cell (Figure 6c, R). Reproducible topographic features were determined by combining the computed surface reliefs (Smith and Kistler, 1977; Guckenberger, 1985) of five well ordered lattices shadowed from different directions (Figure 7). The square unit cell disclosed three structural units: (i) a prominent elongated elevation, (ii) a deep, cross-shaped depression, and (iii) an intermediate unit with three small protrusions of different heights arranged around a central indentation. Superposition of the reaction centre boundaries from the negatively stained unit cell of Figure 5c showed that the pronounced cross-shaped depression correlated with the lipid moiety between PSI complexes (Figure 7a). In addition, these contours identify the top and bottom surfaces of *Synechococcus* sp. reaction centres, which are also discernible in the perspective representation of the membrane surface (Figure 7b).

Projections of PSI complexes from the P1 (class 1), $P2_1$ and P3 lattices as well as that from solubilized reaction centre trimers are displayed at identical magnification and orientation in Figure 8a. The reaction centres embedded in the lipid bilayer exhibited a length of 12.5 ± 0.8 nm and a breadth of 6.5 ± 0.7 nm, which were significantly smaller than those of the reaction centre in the solubilized trimeric complex. It was of interest to note that the small and large hexagonal unit cell dimensions of the *P.laminosum* lattices are related to one another by approximately $\sqrt{3}$, while the unit cell size of the square lattice from *Synechococcus* sp. reaction centres corresponded closely to the length of the PSI complex. This implies that one or the other lattice type can be obtained by a simple rearrangement of the elongated diamond-shaped units, as illustrated in Figure 8b.

The photosynthetic activity of the reconstituted preparations was tested by following light-induced absorption changes due to electron transfer. The magnitude of the bleaching at 700 nm, which is related to the photo-oxidation

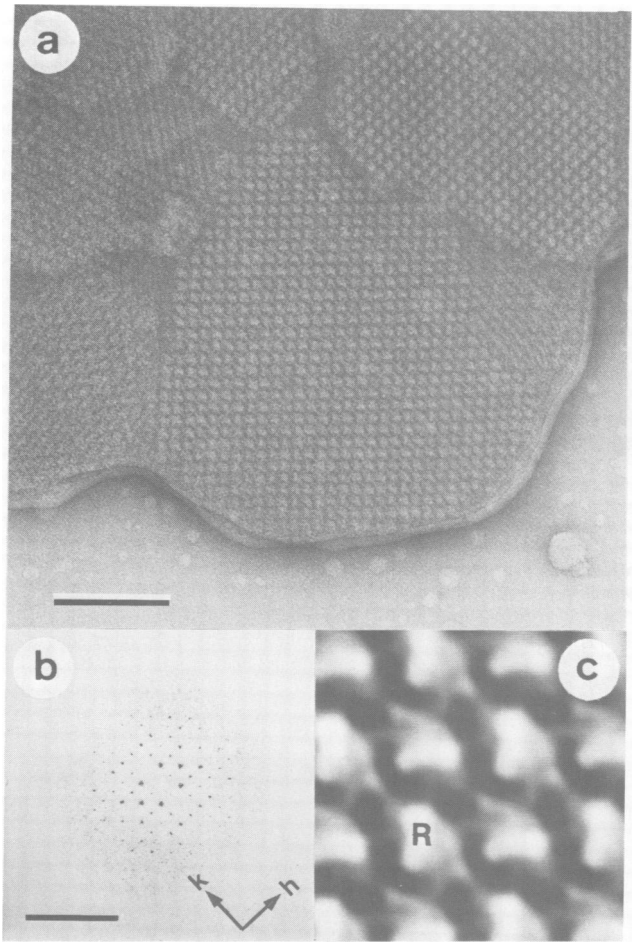

Fig. 5. Square lattices with a unit cell size of 14.5 nm were obtained by dialysis of OBTG from a mixture of solubilized *Synechococcus* sp. reaction centres and lipids in a buffer containing 50 mM $MgCl_2$. These mosaic lattices were usually stacked as double or multiple-layers (**a**). Although the crystalline patches were rather small, they were sometimes well ordered as indicated by 6,2 diffraction spots (**b**). The unsymmetrized correlation average in (**c**) displays elongated reaction centres with a prominent ridge (R) running at ~30° with respect to the axis of the complex. Every other reaction centre is rotated by π about the two-fold symmery axis in the plane of the membrane and shifted by half a unit cell, indicating a $P2_111$ crystallographic packing arrangement. The scale bars represent 100 nm in (a) and $(2\ nm)^{-1}$ in (b).

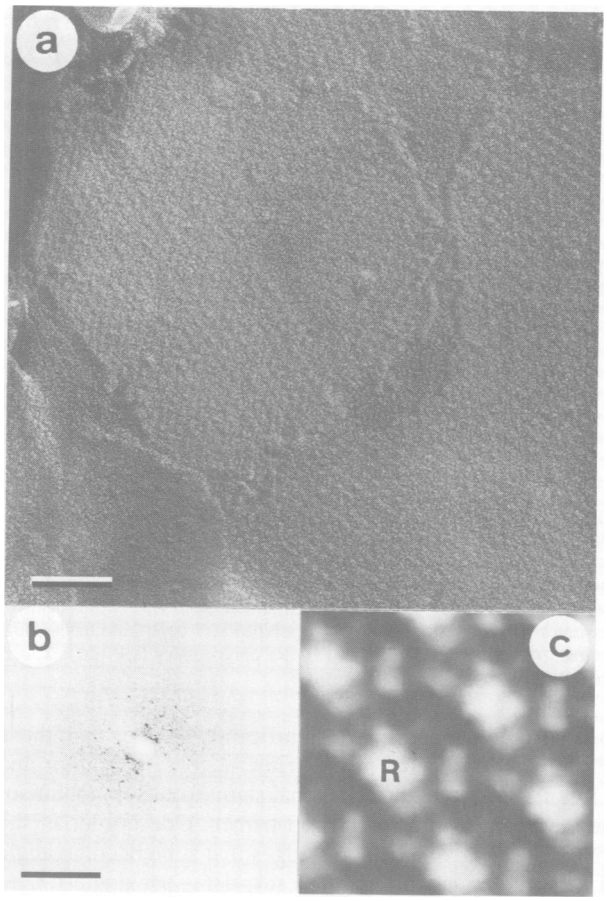

Fig. 6. Freeze-dried metal-shadowed square lattices from *Synechococcus* sp. reaction centres unveiled strongly modulated surfaces (**a**) and diffraction patterns (**b**) with sharp spots up to a resolution of 3 nm. Depending on the shadowing direction, the unit cell morphology varied, but exhibited always one major protrusion (R), one prominent indentation and several small elevations in the intermediate area (**c**). The scale bars represent 100 nm in (a) and $(3\ nm)^{-1}$ in (b).

of the primary electron donor (P700), was taken as an indication of the activity of the complex. In addition, the ability of a membrane-impermeable electron donor (cytochrome *c*) to reduce P700 was used as an indication of the 'sidedness' of the reconstitution (Racker *et al.*, 1975; Orlich and Hauska, 1980). For densely packed but disordered lipid reaction centre vesicles it was found that reconstitution led to a 10–50% loss of activity with *P. laminosum* material, depending on the reconstitution conditions. For crystalline membrane arrays on the other hand, we found a high accessibility (>90%) of P700 to cytochrome *c*, and a higher activity on average than with disordered vesicles. Reconstitutions involving *Synechococcus* sp. material yielded a very high activity (>90% of the original activity), which may be a reflection of the highly thermophilic nature of this strain.

Discussion

Although several 3-D crystals of the photosystem I (PSI) reaction centre have been obtained in the past (Ford *et al.*, 1987, 1988; Witt *et al.*, 1988), and both large subunits (83 kd) have been sequenced (Fish *et al.*, 1985; Cantrell and Bryant, 1987), the sparse structural data so far available has mainly been collected by electron microscopy of negatively stained detergent-solubilized reaction centre trimers (Boekema *et al.*, 1987; Ford and Holzenburg, 1988). Here we demonstrate for the first time that solubilized reaction centres can be crystallized in the presence of phospholipids into highly ordered 2-D lattices by dialysis against detergent-free buffers. Depending on the $MgCl_2$ concentration, several crystallographic packing arrangements have been produced with reaction centres from two thermophilic cyanobacterial species using the detergent OBTG, while with all other detergents tested densely packed, but disordered membranes were obtained. OBTG seemed to have unique properties which allowed the successful preparation of 2-D ordered arrays, suggesting that its inclusion in trials for 2-D crystallization of other membrane proteins should be given high priority.

In spite of the polymorphism, projections of negatively stained reaction centres in different crystallographic packing arrangements revealed similar, elongated complexes of ~12.5 nm length and 6.5 nm breadth, which possessed an asymmetric disposition of a large and a small domain (Figure

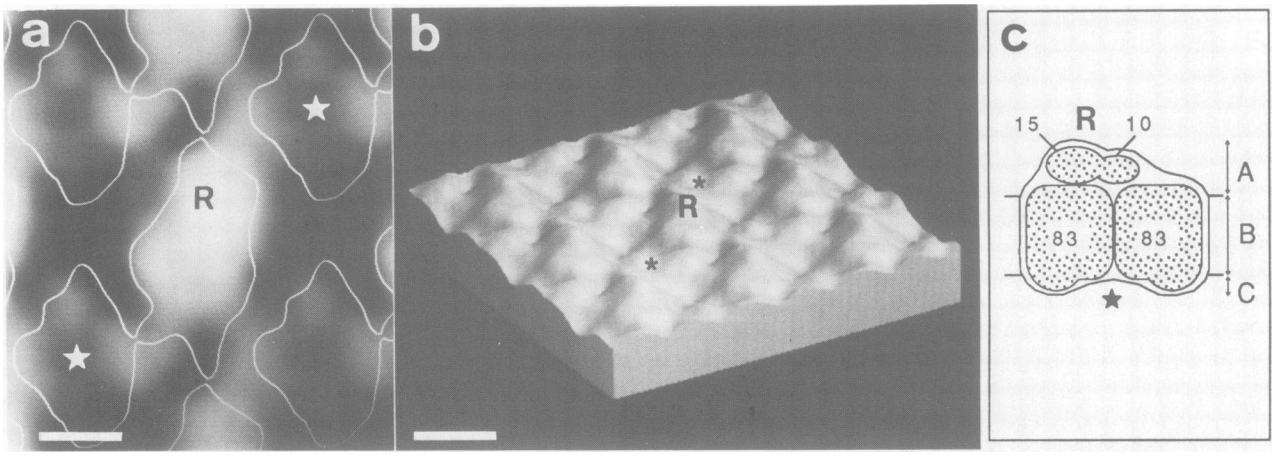

Fig. 7. Five surface reliefs reconstructed from freeze-dried *Synechococcus* sp. reaction centre $P2_1$ lattices shadowed from different directions were aligned and integrated to provide the relief displayed as a 2-D projection in (**a**). The contours of negatively stained $P2_1$ lattices were superimposed to identify top and bottom surfaces of the reaction centres (note that the deviation from $P2_1$ symmetry is due to uneven staining, see text). The perspective view shown in (**b**) reveals a prominent ridge (R) on one side of the reaction centre, whereas the other side is less modulated, exhibiting a central indentation (*) rimmed by three small elevations. Scale bars represent 5 nm in (a) and 10 nm in (b). The schematic cross-section in (c) illustrates how the 10 kd and 15 kd polypeptides contribute to the ridge on one side of the membrane, while the shallow cavity at the other side is assumed to be formed by the two 83 kd polypeptides (see text). The ridge has a height of ~2.5 nm (A), the membrane thickness is 4 nm (B), and the cavity had a depth of ~1 nm (C).

8). These dimensions were significantly smaller than those of the reaction centre of the trimeric form (13.7 nm and 7.8 nm), reflecting the additional stain exclusion volume of the detergent in the solubilized trimer. One border of the complex was defined by two edges that subtended an angle of 120°, thereby explaining the surprising packing arrangement of single reaction centres in the 8.8 nm hexagonal lattice (Figures 2 and 3) as well as their association into trimers during solubilization (Figure 1). The large domain exhibited a ridge of ~6 nm length and 3 nm width emanating from this 120° apex, tapering off towards one end of the reaction centre. The small domain revealed a second, significantly smaller elevation at the other end of all *P.laminosum* PSI complexes, whereas the small domain of the *Synechococcus* sp. reaction centre was less distinct (Figure 8a). This indicated that the PSI complexes from different thermophilic cyanobacteria are not necessarily identical, as also suggested by the different crystallographic packing arrangements (i.e. P1 for *P.laminosum*—but $P2_1$ for *Synechococcus* sp.—material) obtained under the same reconstitution conditions.

The reaction centre was also asymmetric with respect to the plane of the membrane, as demonstrated by freeze-dried metal-shadowed $P2_111$ lattices assembled from *Synechococcus* sp. PSI complexes. Computer reconstructions of their surface reliefs exhibited a prominent ridge on one side of the membrane, whilst the other side appeared to be rather flat, with three small humps embracing a central indentation (Figure 7). This ridge had the same length as that of the large domain, indicating that it is largely the extra mass of this elevation which accounts for the asymmetry of the projected mass distribution of negatively stained complexes. The two classes of projections from the hexagonal P1 lattices reconstituted from *P.laminosum* PSI complexes are compatible with this asymmetry. Capillarity provides for a thorough impregnation of the modulated surface facing the carbon film with staining solution, while the side of the membrane pointing away from the film is not fully stained (Aebi *et al.*, 1976). Therefore, class 1 projections (Figure

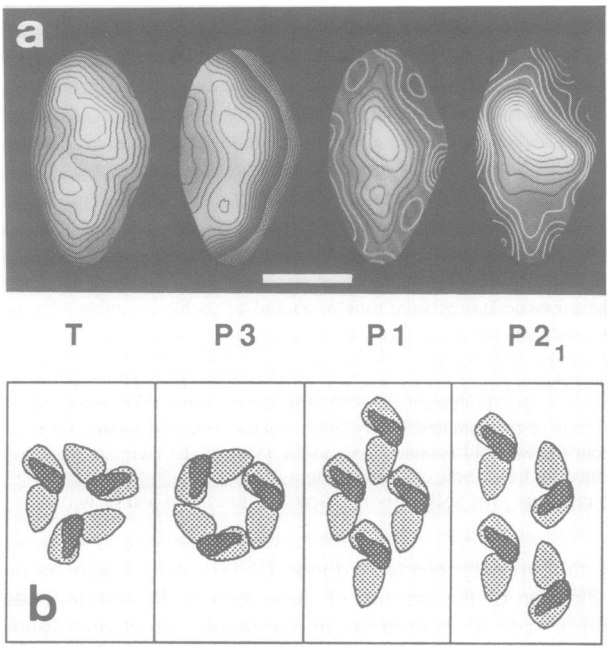

Fig. 8. The projections of negatively stained reaction centres from different packing arrangements are displayed at the same scale in (**a**): solubilized trimer (T); large hexagonal lattice (P3); small hexagonal lattice (P1); square lattice ($P2_1$). The first three are *P.laminosum* reaction centres and the fourth is from *Synechococcus* sp. The projection of the P1 lattice is the sum of four aligned correlation averages from different lattices and includes the projection shown in Figure 3c. A schematic representation of the main features of PSI reaction centres and their packing arrangements is shown in (b). The scale bar in (a) represents 5 nm.

3) were observed when the reaction centres were oriented with respect to the glow-discharged carbon film in the same way as the well preserved solubilized trimers (Figure 1), i.e. the ridge on one side of the reaction centre facing the supporting film. On the other hand, class 2 projections

(Figure 2) were observed when the shallow central indentation on the other side of the reaction centres faced the hydrophilic film. The disposition of a slightly stained pit embraced by a proteinous rim (Figure 2c,*) showed a surprising resemblance to the surface relief from the flat side of *Synechococcus* sp. reaction centres (Figure 7b,*), considering the different origin and the different crystallographic packing arrangement of the complexes, as well as the complementary specimen preparation methods used.

Reaction centres reconstituted into lipid bilayers exhibited a significant retention of their biological activity, as assessed by the bleaching at 700 nm due to the photo-oxidation of P700. We also made an attempt to determine the 'sidedness' of the reconstituted vesicles, i.e. the orientation of the reaction centres within the lipid bilayer, using cytochrome *c* as a membrane impermeable electron donor. For this purpose, the bleaching at 700 nm was first measured with reconstituted reaction centres in lipid bilayers and subsequently after their solubilization by dodecyl maltoside. As reported for other systems (Racker *et al.*, 1975; Orlich and Hauska, 1980) the accessibility of P700 in reconstituted vesicles by cytochrome *c* was highly dependent on the initial conditions and on the nature and concentration of the solutes in the buffer, i.e. on the morphology of the vesicles. Therefore, we could not unambiguously determine the orientation of densely packed, disordered reaction centres in vesicles. For example, a low P700 accessibility was measured in multi-lamellar vesicles that were obtained in the presence of 1 mM Co^{3+}, since the reaction centres in internal membrane spheres of the onion-like vesicles were inaccessible, independent of their orientation in the membrane. Nor could we identify the orientation of the reaction centres in crystalline arrays, because leaky vesicles and/or single- or multi-layered open ended sheets could not be ruled out. Nevertheless, in the context of the structural analysis presented here, the assessment of the biological activity *per se* is crucial in order to document that reconstitution conditions and prolonged exposure to detergents do not impair the function of reaction centres.

Two independent estimates of the reaction centre cross-sectional area in the plane of the membrane can be deduced. With *Synechococcus* sp. reaction centres a lipid to protein ratio (LPR; w/w) of at least 0.25 was required to grow well ordered lattices. From this we estimate that 35% of the $P2_1$ unit cell area must be occupied by the lipid moiety, leaving a cross-sectional area of 68 nm^2 per reaction centre. In contrast, a smaller amount of DMPC was incorporated in the hexagonal lattices from *P.laminosum* PSI complexes, since protein-free lipid areas were frequently visible on vesicles reconstituted from DMPC and *P.laminosum* PSI complexes with an LPR of 0.25 (see Figure 3 and 4). The surface area occupied by one reaction centre plus lipid moiety was 67 nm^2 and 72 nm^2 for the small and large hexagonal lattices, respectively, reflecting the $\sqrt{3}$ relationship of the lattice vectors. Assuming that 15% of the unit cell area was covered by lipid molecules in these hexagonal lattices, the reaction centre areas of *P.laminosum* complexes come to 57 nm^2 or 61 nm^2, respectively. This yields an average cross-sectional area of 62 $\pm$ 5 nm^2 per reaction centre, as calculated from the three packing arrangements. Alternatively, we calculate the cross-section of the PSI complex to be 64 nm^2 taking the average length (12.5 nm) and width (6.5 nm) of the elliptical complex. The volume occupied by protein plus chlorophyll *a* and carotenoid molecules within the 4 nm thick DMPC bilayer then amounts to 252 nm^3 corresponding to 209 kd, which includes ~62 kd for the 60–70 light-harvesting molecules and twice 74 kd for the membrane spanning segments of the two 83 kd polypeptides. This implies that the partially inactive form of the reaction centre, the CP-1 complex, consisting of the two 83 kd polypeptides only (Takahashi *et al.*, 1982; Ford, 1987), has not more than 9 kd per subunit protruding into the aqueous environment. Thus, it is likely that the pronounced asymmetry of the reaction centre is due to the more hydrophilic 10 kd and 15 kd polypeptides (Figure 7c). Assuming to a first approximation that their mass is arranged in a cylinder of 6 nm length (see above), we estimate the height of the ridge to be 2.5 nm.

It is also interesting to compare the structural data presented here with predictions made from sequence data which led to the proposal that each of the two 83 kd subunits of ~750 residues contains 11 membrane spanning α-helices (Fish *et al.*, 1985; Cantrell and Bryant, 1987). On this basis, one would expect a dumb-bell shaped complex with only ~40% of its protein mass in the membrane, and with extended hydrophilic domains on each side. Clearly this model is in stark contrast with our electron microscopy data and other biophysical measurements (Haworth *et al.*, 1982). As an α-helix has one residue per 0.15 nm axial rise, its mass per length is ~0.74 kd/nm. Considering that 74 kd of one 83 kd polypeptide are in the membrane and hence probably in α-helical form, we calculate a total length of 100 nm or 25 membrane spanning α-helical segments per subunit. Alternatively, we can estimate that ~45 nm^2 of the reaction centre cross-sectional area is occupied by membrane spanning polypeptide segments, the remainder accounting for bound chlorophyll and carotenoid. This yields 25 α-helices per 83 kd subunit as well, if the published value for the bacteriorhodopsin α-helix cross-section of 0.8–1 nm^2 (Hayward and Stroud, 1981) is taken. The value of 25 α-helices is based on the assumption that the helices run perpendicularly across the membrane and are densely packed. Alternatively, α-helical cross-sectional areas of 0.5–2 nm^2 have been estimated, taking extremes of amino acid residue sizes (Tamm, 1986). Taking such extreme values, 11–45 membrane spans are calculated, indicating that the number predicted from the sequence data represents a lowest limit.

In summary, it would be reasonable to look for further membrane spans in the sequences of the two large subunits. Indeed, inspection of the alignment of the sequences in the paper of Cantrell and Bryant reveals several areas of >18 amino acids where charged residues are excluded. In the *psaA* gene product, stretches between amino acid residues 481 and 519, 633 and 654, and 657 and 672 can be identified, whilst in the *psaB* product areas between positions 107 and 133, 218 and 238, 241 and 266, and 624 and 643 stand out. This interpretation of the sequence data would suggest that the symmetrical arrangement of membrane spans is broken, as only one of the newly proposed membrane spans is found in both 83 kd polypeptide chains.

The structural model of the PSI reaction centre emerging from the data presented here envisages a complex assembled from two membrane resident 83 kd polypeptide which bind the 60–70 light-harvesting molecules and form a central, shallow cavity on one side of the membrane. The distinct asymmetry of the complex appears to be due to the 10 kd and 15 kd subunits bound to the 166 kd dimer at the other

side of the membrane. Here we speculate that the two smaller polypeptides together form the ridge of the large morphological subunit, as indicated schematically in Figures 7c and 8b. This would allow the final iron–sulphur centres A and B of the 10 kd polypeptide to be positioned over the interface between the two 83 kd polypeptides, to which the locus of electron transport has tentatively been assigned (Golbeck *et al.*, 1987). In addition, this exposed position would permit a ready association with further water soluble electron transfer proteins (ferredoxin, ferredoxin-NADP reductase). However, a structural asymmetry due to a different fold of the similar but not identical 83 kd polypeptides cannot be excluded. Furthermore, an association of one small polypeptide per 83 kd subunit could also be possible. In the long run, X-ray structural analysis will clarify these questions, although a comparative electron microscopical analysis of lattices assembled from CP-1 complexes might provide quicker answers.

Materials and methods

Chemicals

Dimyristoyl phosphatidylcholine (DMPC) and horse heart cytochrome *c* were purchased from Sigma, the detergents dodecyl maltoside, octyl-β-D-glucopyranoside (OBG), octyl-β-D-thioglucopyranoside (OBTG), sodium deoxycholate (DOC) were purchased from Calbiochem. Polyethyleneglycol (PEG) 6000 was purchased from Merck. Octyl-polyoxyethylene (octyl-POE) was a kind gift of Dr J.Rosenbusch, Biocentre, University of Basel. All other chemicals used were of analytical grade.

Detergent extraction and isolation

The photosystem I reaction centres from *P.laminosum* clone OH-1 were obtained as described previously (Ford *et al.*, 1988). Reaction centres from *Synechococcus* sp. clone OD24 (Miller *et al.*, 1988) were isolated from photosystem II-depleted membranes (kindly provided by Drs M.Miller and R.P.Cox, Odense University, Denmark). The membranes were suspended at 2 mg chl *a*/ml in a buffer containing 10 mM HEPES, 5 mM K_2HPO_4, 10 mM $MgCl_2$ and 25% glycerol, pH 7.5. Dodecyl maltoside was added slowly to a concentration of 1.67% w/v from a 10% w/v stock solution, and then the sample was incubated for 5 min at 37°C. After centrifugation for 2 min at 14 000 *g*, the supernatant, which contained ~80% of the Chl, was subjected to a fractional precipitation with PEG 6000 at a concentration of 1–10% in the presence of 70 mM $MgCl_2$. Precipitated material was pelleted for 20 min at 22 000 *g*. The fraction between 4.5 and 6% (w/v) PEG 6000 was resuspended in the same buffer and then transferred to a Sepharose-CL 6B column (70 cm long, 2.5 cm diameter) for elution at 2 ml/h. The running buffer consisted of 10 mM HEPES, 5 mM K_2HPO_4, 150 mM NaCl, and 0.05% dodecyl maltoside, pH 7.5. The column separated the green coloured material into two bands which were determined to be trimer and monomer by analytical SDS–PAGE under non-denaturing conditions (Ford, 1987). The fractions containing trimeric complexes were pooled and concentrated by a precipitation with PEG 6000 (8% w/v) and $MgCl_2$ as described above. Protein and chlorophyll were determined as described previously (Ford *et al.*, 1982).

Reconstitution

Isolated reaction centre trimers were mixed with detergent–phospholipid mixed micelles and reconstituted into membranes by detergent removal in a continuous flow dialysis system (Engel *et al.*, 1988). DMPC was solubilized with several detergents [dodecyl maltoside (0.2% w/v), DOC (1% w/v), OBG (2% w/v), OBTG (1% w/v) octyl-POE (1% w/v), and SDS (0.2% w/v)], all materials used without further purification. For the reaction centres, the exchange of dodecyl maltoside for one of the other detergents was achieved by PEG 6000/$MgCl_2$ precipitation followed by resuspension in the new detergent-containing buffer (10 mM HEPES, pH 7.0). This precipitation/resuspension procedure was repeated three times. Detergent concentrations were adjusted to the values given above except with OBTG (0.5% w/v). The protein concentration in the final reconstitution mixture (0.3 ml) was 1.6 mg/ml and the lipid concentration was 0.4 mg/ml, giving a lipid to protein ratio (LPR) of 0.25. In experiments where the LPR was changed (see Discussion), the lipid concentration was varied. The reconstitution buffer (10 mM HEPES, pH 7.0, with a variable concentration of $MgCl_2$ or other salts as described in the Results and Discussion) was pumped through the dialysis cell reservoir at 1 ml/min, yielding a complete replenishment of the reservoir every minute. The dialysis cell temperature was adjusted to 25°C for the first 12 h and it was increased linearly during the next 12 h to 37°C. After 20–24 h a similar temperature ramp brought the sample back to 25°C, giving a total dialysis time of up to 60 h.

Activity measurements

Activity of the reaction centre material was tested with an Aminco DW-2 spectrophotometer as described previously (Ford, 1987), using horse heart cytochrome *c* pre-reduced with 1 mM sodium ascorbate as electron donor. After resolubilization of the membranes with 0.1% w/v dodecyl maltoside, dichlorophenol indophenol was added to a final concentration of 100 μM.

Electron microscopy

Reconstituted protein–lipid membranes were adsorbed to carbon coated parlodion films that were mounted on electron microscope grids and rendered hydrophilic by glow discharge at low pressure in air. After washing in Tris buffer (10 mM, pH 7) the membranes were negatively stained with 0.75% uranyl formate (pH 4.2). To obtain information on their surface structure, adsorbed membranes were washed in double-distilled water, frozen in liquid nitrogen, freeze-dried in a Balzer BAF 300 unit at −80°C and unidirectionally shadowed with tantalum–tungsten at an elevation angle of 30°C at the same temperature. Images were recorded on Kodak SO-163 film at a nominal magnification of 50 000× under low-dose conditions using a Hitachi H-7000 transmission electron microscope operated at 100 kV. The magnification was calibrated with negatively stained catalase crystals as described by Wrigley (1968). Micrographs were selected by optical diffraction (Aebi *et al.*, 1973) according to the crystallinity of reconstituted membranes and a correct alignment of the microscope.

Image processing

Suitable areas were digitized using an Eikonix 850 CCD camera equipped with a Zeiss S planar objective lens. To eliminate noise introduced by gain and bias variations of the CCD-array, an empty frame was recorded and stored for on-line normalization. In addition, 3 × 3 pixel areas were averaged and stored as single pixels separated by ~0.64 nm. Two methods were applied for calculating averaged projections of reaction centre unit cells using the SEMPER image processing system (Saxton *et al.*, 1979). Firstly, quasi-optical Fourier peak filtration (Aebi *et al.*, 1973) was used for a rapid evaluation of unit cell morphologies and crystal quality. Secondly, correlation averaging (Saxton and Baumeister, 1982) allowed the elimination of residual lattice disorder by locating the unit cells precisely using a reference that included three to four PSI complexes. To separate stacks of superimposed, angularly aligned 2-D lattices, the single-layer motif M_1 was estimated from the multiple-layer motif M_2 using Eq. 1, assuming that each layer was shifted with respect to its lower neighbour by *x*,*y*:

$$M_1 = M_2 \Sigma \exp(i\Phi_n)/(|\Sigma \cos(\Phi_n)|^2 + |\Sigma \sin(\Phi_n)|^2 + c) \qquad (1)$$

where $\Phi_n(x,y)$ represents the phase shift of the *n*th layer with respect to the first layer, *c* is a constant to be suitably adjusted with respect to the average background noise, and the sums are taken over *N* layers. M_1 was then three-fold symmetrized, a stack of *N* layers was calculated and finally cross-correlated with M_2. The correlation coefficient as well as the deviation from the three-fold symmetry were a convenient measure of the quality of estimate M_1, and were optimized by variation of *x*, *y* and *N*. This procedure was simpler but less versatile than the approach of Kühlbrandt (1988), who did not assume a fixed displacement between the layers.

Surface reliefs were computed from averaged freeze-dried metal-shadowed lattices following the procedure outlined by Smith and Kistler (1977) and Guckenberger (1985).

Single trimeric complexes were aligned angularly either directly or by their autocorrelation function and translationally with respect to a reference for subsequent averaging (Frank *et al.*, 1978). In a first run an arbitrarily chosen trimer served as reference, whereas for subsequent refinement runs the averaged projection was used. To discriminate top and bottom views of these trimers with their threefold axis oriented perpendicularly to the carbon film, an attempt was made to identify those particles that exhibited a higher correlation value with the mirror image of the reference.

Acknowledgements

We are grateful for the generous gift of photosystem II depleted membranes from Drs M.Miller and R.P.Cox of the Institute of Biochemistry, Odense University, Denmark. We thank Dr A.Holzenburg and Andreas Hoenger for electron microscopy of detergent solubilized reaction centre trimers and reconstituted disordered membranes in the early stages of this work. Josef

Wey is thanked for his technical assistance and Professor J.Rosenbusch for kindly providing the octyl-POE. We are indebted to Professor U.Aebi for his continuous support and for fruitful discussions. This project was supported by grant No. 31-25684.88 (to A.Engel) and grant No. 3.528-0.86 (to R.Ford) awarded by the Swiss National Foundation for Scientific Research, the M.E.Müller-Foundation of Switzerland, and the Department of Education of the Kanton Basel-Stadt.

References

Aebi,U., Smith,P.R., Dubochet,J., Henry,C. and Kellenberger,E. (1973) *J. Supramol. Struct.*, **1**, 498–522.

Aebi,U., Bijlenga,K.L., ten Heggeler,B., Kistler,J., Steven,A.C. and Smith,P.R. (1976) *J. Supramol. Struct.*, **5**, 475–495.

Bengis,C. and Nelson,N. (1975) *J. Biol. Chem.*, **250**, 2783–2788.

Boekema,E.J., Dekker,J.P., van Heel,M.G., Roegner,M., Saenger,W., Witt,I. and Witt,H.T. (1987) *FEBS Lett.*, **217**, 283–286.

Cantrell,A. and Bryant,D.A. (1987) *Plant Mol. Biol.*, **9**, 453–468.

Engel,A., Holzenburg,A., Stauffer,K., Rosenbusch,J.P. and Aebi,U. (1988) *Proceedings of the 46th Annual Meeting of the Electron Microscopy Society of America.* Bailey,G.W. (ed.), San Francisco Press, Inc, pp. 152–153.

Fish,L.E., Kück,U. and Bogorad,L. (1985) *J. Biol. Chem.*, **260**, 1413–1421.

Ford,R.C. (1987) *Biochim. Biophys. Acta*, **849**, 16–24.

Ford,R.C. and Holzenburg,A. (1988) *EMBO J.*, **7**, 2287–2293.

Ford,R.C., Chapman,D.J., Barber,J., Pedersen,J.Z. and Cox,R.P. (1982) *Biochim. Biophys. Acta*, **681**, 145–151.

Ford,R.C., Picot,D. and Garavito,R.M. (1987) *EMBO J.*, **6**, 1581–1586.

Ford,R.C., Pauptit,R.A. and Holzenburg,A. (1988) *FEBS Lett.*, **238**, 385–389.

Frank,J., Goldfarb,W., Eisenberg,D. and Baker,T.S. (1978) *Ultramicroscopy*, **3**, 283–290.

Golbeck,J.H., McDermott,A.E., Jones,W.K. and Kurtz,D.M. (1987) *Biochim. Biophys. Acta*, **891**, 94–98.

Guckenberger,R. (1985) *Ultramicroscopy*, **16**, 357–370.

Haworth,P., Tapie,P., Arntzen,C. and Breton,J. (1982) *Biochim. Biophys. Acta*, **682**, 152–159.

Hayward,S.B. and Stroud,R.M. (1981) *J. Mol. Biol.*, **151**, 491–517.

Hoj,P.B., Svendsen,I., Scheller,H.V. and Moller,B.L. (1987) *J. Biol. Chem.*, **262**, 12676–12684.

Kühlbrandt,W. (1988) *J. Mol. Biol.*, **202**, 849–864.

Miller,M., Pedersen,J.Z. and Cox,R.P. (1988) *Biochim. Biophys. Acta*, **943**, 501–510.

Morschel,E. and Schatz,G.H. (1987) *Planta*, **172**, 145–154.

Orlich,G. and Hauska,G. (1980) *Eur. J. Biochem.*, **111**, 525–533.

Racker,E., Knowles,A.F. and Eytan,E. (1975) *Annals NY. Acad. Sci.*, **264**, 17–33.

Rutherford,A.E. and Heathcote,P. (1985) *Photosynthesis Res.*, **6**, 295–316.

Saxton,O.W., Pitt,T.J. and Horner,M. (1979) *Ultramicroscopy*, **4**, 343–354.

Saxton,O.W. and Baumeister,W. (1982) *J. Microsc.*, **127**, 127–138.

Smith,P.R. and Kistler,J. (1977) *J. Ultrastruct. Res.*, **61**, 124–133.

Takahashi,Y., Koike,H. and Katoh,S. (1982) *Arch. Biochem. Biophys.*, **219**, 209–218.

Tamm,L.K. (1986) *Biochemistry*, **25**, 7470–7476.

Witt,I., Witt,H.T., DiFiore,D., Rögner,M., Hinrichs,W., Saenger,W., Granzini,J., Betzel,C. and Dauter,Z. (1988) *Ber. Bunsenges. Phys. Chem.*, **92**, 1503–1506.

Wrigley,N.G. (1968) *J. Ultrastruct. Res.*, **24**, 454–464.

Received on June 13, 1990; revised on July 12, 1990